

Analysis of Vehicle Lateral Dynamics due to Variable Wind Gusts

Youhanna William, Walid Oraby, and Sameh Metwally
Helwan University

ABSTRACT

This study presents a practical theoretical method to judge the aerodynamic response of buses in the early design stage based on both aerodynamic and design parameters. A constant longitudinal velocity 2-DOF vehicle lateral dynamics model is used to investigate the lateral response of a bus under nine different wind gusts excitations. An appropriate 3-D CFD simulation model of the bus shape results is integrated with carefully chosen design parameters data of a real bus chassis and body to obtain vehicle lateral dynamic response to the prescribed excitations.

Vehicle model validity is carried out then, the 2-DOF vehicle lateral dynamics model has been executed in MATLAB Simulink environment with the selected data. Simulation represents the vehicle in a straight ahead path then entered a gusting wind section of the track with a fixed steering wheel. Vehicle response includes lateral deviation (LD), lateral acceleration (LA), yaw angle (YA) and yaw rate (YR). Results showed that in case of 25 m/s wind gust [which corresponds to 45° wind relative yaw angle (β_w)], the vehicle Lateral Deviation (LD) maintained about 5 m after 4.5 seconds of entering the wind gust. Moreover, vehicle Yaw Rate (YR) reaches a maximum value of about 2.3deg/s during such maneuver simulation time.

CITATION: William, Y., Oraby, W., and Metwally, S., "Analysis of Vehicle Lateral Dynamics due to Variable Wind Gusts," *SAE Int. J. Commer. Veh.* 7(2):2014, doi:10.4271/2014-01-2449.

1. INTRODUCTION

When driving a vehicle on the road, the driver has to compensate continuously for small directional deviations from the desired course due to disturbances such as crosswinds and road irregularities leading to unintended path deviation. With higher and larger side area such as buses and trucks, the influence of crosswind on the vehicle lateral dynamics behavior is much higher and the vehicle becomes more sensitive to side wind excitations.

In a real case for such non-steady motion of a vehicle, the aerodynamic loads influence its directional stability and overall safety. Prototype vehicles have been used to check vehicle stability by actual driving tests to evaluate the effect of transient aerodynamics. However at this stage it is often too late to make changes to neither vehicle shape nor vehicle chassis design parameters [1]. In order to reduce the cost of developing a new vehicle and allow early intervention, much research activity has involved developing handling and stability simulations to study the effect of aerodynamics during the early design phase. The aerodynamic models used in such simulations are determined from experimental quasi-steady wind tunnel tests performed on full scale vehicle shape model, or on a scaled one [1].

However the essential crucial way to judge the crosswind stability of a vehicle is through experiments, numerical simulations are more flexible to set up and design compared to experiments [2]. In the last decade, many researchers have investigated the aerodynamic characteristics of ground vehicles using CFD techniques [3,4,5] and they concluded that CFD is a strong tool to assess ground vehicle aerodynamics in primary design stages. The present work goal is to introduce a proper integration between CFD results for 3-D bus shape model and the mathematical model that represents vehicle lateral dynamics. The main lateral dynamics parameters of a vehicle that have an impact on its response are reported in details.

2. CFD SIMULATION METHODOLOGY

2.1. Bus Model Simulation Objectives

In order to determine the aerodynamic characteristics (which is essential for the mathematical modeling); a 3-D CFD simulation of bus model has performed using the industrial software ANSYS-Fluent 14.0 [6]. The numerical simulation strategy is to impose a resultant wind velocity (V_w) with variable magnitudes and directions of wind relative yaw angle (β_w) to simulate the variation in crosswind gusts from 2.187 m/s at $\beta_w = 5^\circ$ to 25 m/s wind velocity at $\beta_w = 45^\circ$. The magnitude of crosswind gusts is relatively changed with each angle of (β_w)

according to the value of resultant wind velocity lateral component ($V_w \sin \beta_w$) (which represents lateral wind gust velocity (V_l)) as shown in (Figure 1). The studied range is from $\beta_w = 5^\circ$ to $\beta_w = 45^\circ$ with step 5° . That has been applied to the 3-D bus model with constant upwind speed 25 m/s.

All the details of CFD simulation (bus model design, grid independence study, turbulence model investigation and selection, computational domain dimensions and shape, final grid settings, obtained velocity contours, and surface pressure distribution) are presented by William, Y.E. et al [7]. The major CFD parameters are mentioned in (Table 1).

Table 1. Major CFD parameters.

Turbulence Model	Realizable k-ε
Discretization Scheme	Second-order upwind scheme for all variables
Solving Algorithm	Semi-implicit method for pressure linked equation (SIMPLE)
Number of Elements	10.9 Million (approximately)
Maximum Residual for All Parameters	10^{-4}

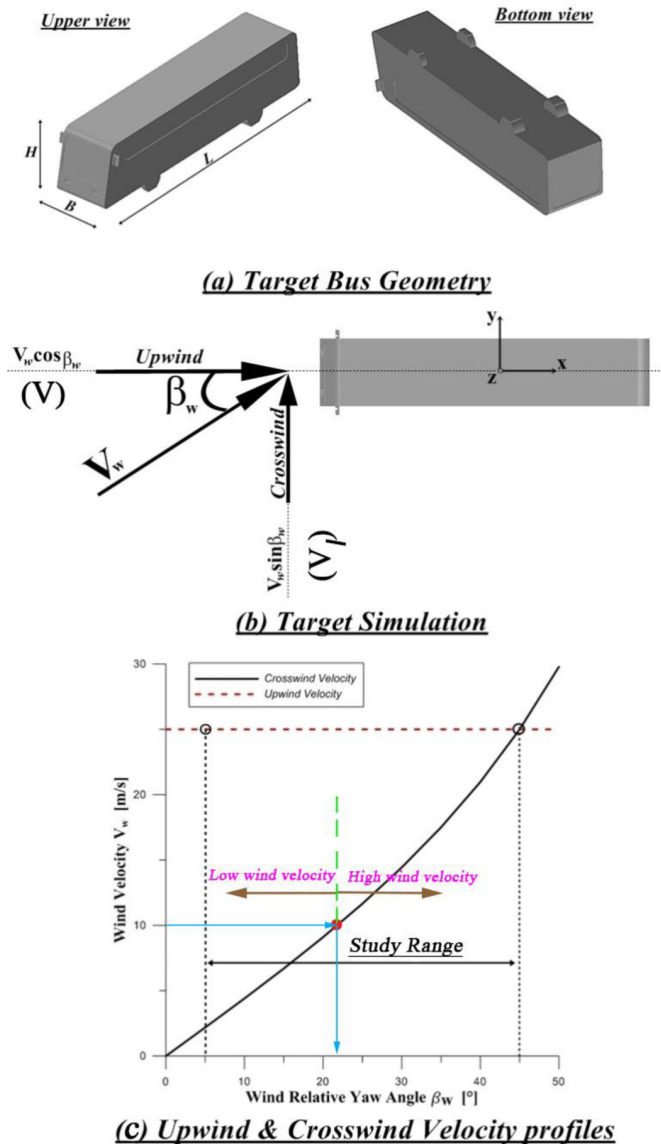


Figure 1. Overview of target bus geometry and simulation strategy.

2.2. CFD Obtained Results

However the six aerodynamic components are reported from the CFD simulation, only side force (F_s) and its aerodynamic center (AC) position are required to perform the 2-DOF vehicle lateral dynamics mathematical modeling simulation. Side force (F_s) parameters which are demonstrated in Eq.(1&2) are important to understand the produced side force (F_s) from each wind gust. From five influencing parameters on the value of wind gust side force (F_s), only two are changing during CFD simulation (which are side force Coefficient (C_s) and lateral wind gust velocity (V_l)).

$$F_s = 0.5 * \rho_{air} * A_f * C_s * V_w^2 \tag{1}$$

And (V_w) can be expressed as:

$$V_w^2 = V^2 + V_l^2 \tag{2}$$

Each wind gust has a specific three characteristics (which are side force Coefficient (C_s), lateral wind gust velocity (V_l), and distance between vehicle aerodynamic center (AC) and its rear end (L_w). However, the side force coefficient (C_s) is directly proportional with lateral wind gust velocity (V_l), the aerodynamic center distance (L_w) has another behavior. With increasing of wind relative yaw angle (β_w)(which corresponds lateral wind gust velocity(V_l), a huge pressure difference is generated between bus model two side surfaces.

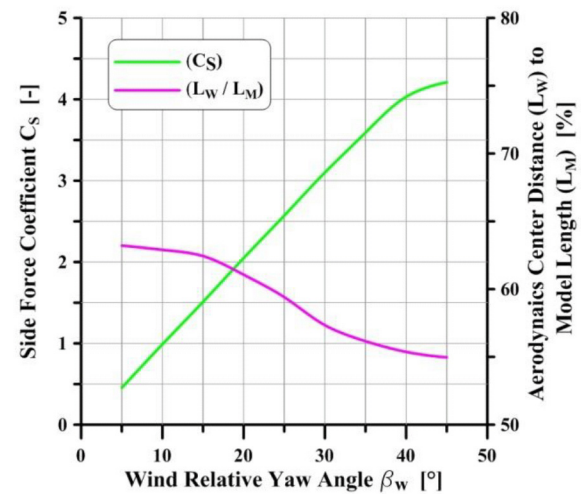


Figure 2. Variation of side force coefficient and aerodynamic center distance with (β_w).

Side force coefficient (C_s) value is depending on this pressure difference which explains the rising tendency of the curve. The aerodynamic center (AC) position is changing according to the change in pressure distribution of air on bus model all surfaces. Due to increasing in lateral wind gust velocity (V_l), the pressure stagnation area (the sum of stagnation points and lines at which the static pressure has its maximum value) of bus model side surfaces is increasing. Moreover, the position of

aerodynamic center (AC) changed by lateral wind gust is shifted to be more closer to bus model rear end as shown in (Figure 2).

3. VEHICLE LATERAL DYNAMICS MODELING

3.1. Vehicle Motion in Lateral Wind Gust

A simple 2-DOF lateral dynamics model is used to determine the vehicle lateral response due to variable wind gusts. The used model is presented by Abe, M. [8] and Hucho, W.H. [9], however, with a little modification as presented in Eq.(3&4). In order to fit the used mathematical model with bus criteria, each (K_r) is replaced by ($2K_r$) as a result of four wheels in the vehicle rear axle existence. The established model considers situation where vehicle is traveling straight ahead ($\delta=0$) with a constant velocity ($V=$ Constant) (V also represents upwind velocity during CFD simulation in which the vehicle is assumed to be stationary and air is moving), then, subjected to a sudden lateral wind gust with velocity (V_l). A side force (F_s) is generated which acts at the vehicle AC. The distance between vehicle CG and vehicle AC is (l_w).

$$m \frac{d^2 y}{dt^2} + \frac{2(K_f + 2K_r)}{V} \frac{dy}{dt} + \frac{2(l_f K_f - 2l_r K_r)}{V} \frac{d\theta}{dt} - 2(K_f + 2K_r)\theta = F_s \quad (3)$$

$$I \frac{d^2 \theta}{dt^2} + \frac{2(l_f K_f - 2l_r K_r)}{V} \frac{dy}{dt} + \frac{2(l_f^2 K_f + 2l_r^2 K_r)}{V} \frac{d\theta}{dt} - 2(l_f K_f - 2l_r K_r)\theta = -l_w F_s \quad (4)$$

As a result of vehicle tires cornering stiffness, an internal lateral vehicle force is produced which is ($2\beta(K_f + 2K_r)$). This force is acting in the vehicle neutral steer point (NSP) as shown in (Figure 3). The distance between vehicle CG and vehicle NSP is (l_N). Both of (l_N) and (l_w) are taken as positive if the NSP and AC are behind the vehicle CG. Actually (l_N), which is shown in Eq.(5) determines the vehicle handling behavior (i.e. under/over steer). However, in such simulation the investigated vehicle response will be quite different. Regarding current simulation conditions, either clockwise (CW) or counterclockwise (CCW) settling yaw motion of vehicle CG is the main expected behavior.

$$l_N = -\frac{(l_f K_f - 2l_r K_r)}{K_f + 2K_r} \quad (5)$$

The lateral wind gust scenarios proposed to simulate the standard Volkswagen crosswind facility [9]. This (47 m) length side wind facility is assumed to affect the vehicle after half a second of entering the facility. In other words, the lateral wind gust excitation is applied after half a second from simulation start point. The wind gust profile maintained at its maximum value after (8 m) of wind gust initialization at the beginning of

wind facility. The same distance is taken to collapse wind gust from its maximum value to zero at the end of crosswind facility. The overall wind gust duration is 1.88 seconds as shown in (Figure 4) provided that vehicle longitudinal velocity, while passing this facility, is kept at 90 km/hr. In fact, the effect of crosswind on road vehicles had been studied by similar wind gust excitations as used by [1,9,10,11].

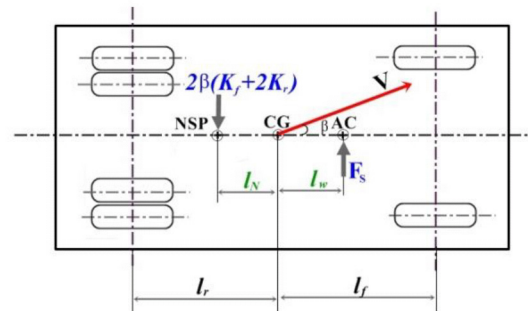


Figure 3. Bus model with existed lateral forces.

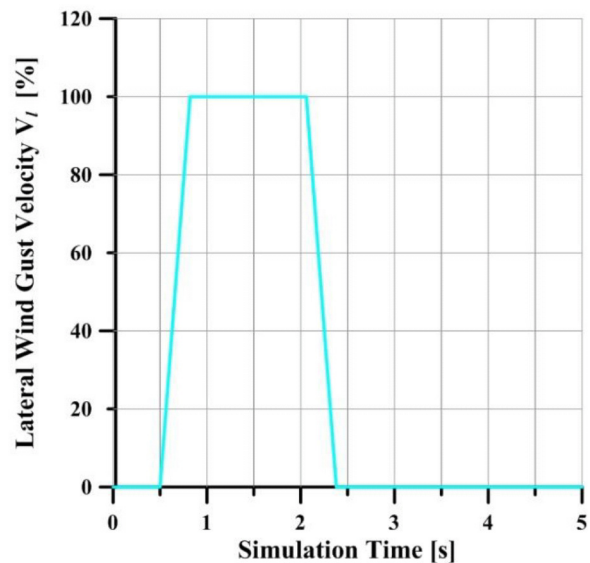


Figure 4. Lateral wind gust velocity profile.

3.2. Model Validation

Before starting in bus model lateral dynamics simulation and analysis, it was essential to judge the executed model in MATLAB Simulink [12] environment validity. A sample yaw rate (YR) response of the concluded results is compared with its parallel response reported by Abe, M. [8]. A typical vehicle chassis parameters and aerodynamic lateral wind gust excitation conditions is used. The comparison of the obtained results (Figures 5,6) has shown an identical vehicle response behavior. Which emphasizes the validity of the executed model before modifying it to be relevant with bus model simulation ($(2K_r)$ instead of (K_r)).

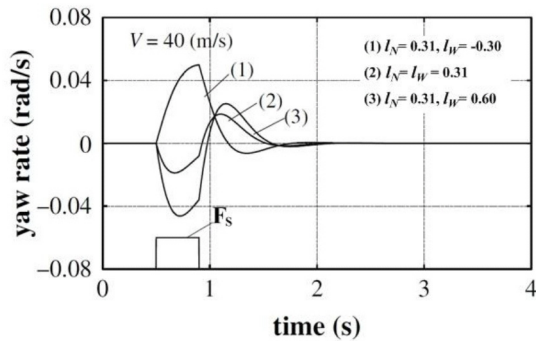


Figure 5. Vehicle yaw rate response due to lateral wind gust reported by Abe, M. [8].

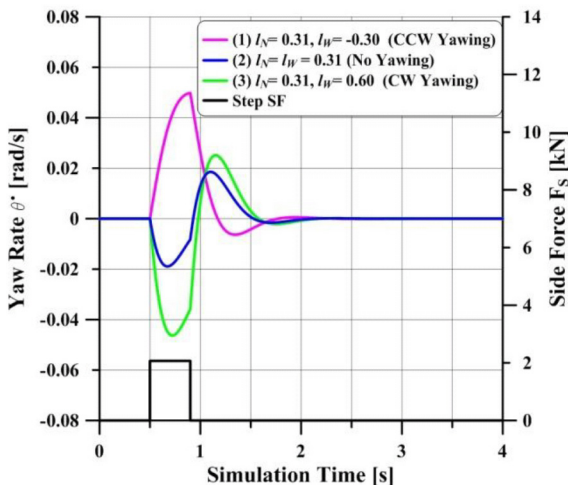


Figure 6. Obtained vehicle yaw rate response due to lateral wind gust.

4. BUS MODEL SIMULATION DATA

Two types of data are required to perform simulation, i.e., chassis design data and aerodynamics data. The chassis data are parameters which assumed to be constant while carrying out the simulation (e.g., axle normal load, bus CG position, tire cornering stiffness). A carefully chosen bus chassis design parameters data is used as mentioned by [13]. Bus shape model length (L_M) and frontal area (A_f) is used with a proper scale to be compatible with other parameters. In order to fulfill bus chassis parameters data, a Michelin tire model is used to represent normal load versus cornering stiffness relationship for the proposed tire size 11.00"/80 R 22.5" as shown in (Figure 7) [14]. Bus chassis parameters data represent full load chassis with its corresponding axle load distribution. The tire normal load is employed to determine its cornering stiffness. The full bus chassis design parameters data are shown in (Table 2).

Regarding bus aerodynamic parameters, for each wind relative yaw angle (β_w) (which corresponds lateral wind gust velocity (V_f)) two parameters are changed respectively. Basically, the variable parameters are side force coefficient (C_s) and distance between vehicle GC and AC (l_w). Values for such bus body

shape had been concluded from CFD simulations study [Z]. All the reported CFD values of (l_w) are found to be in front of bus CG, i.e., its values are substituted with negative sign (-) in the executed MATLAB Simulink model during simulation. All bus model aerodynamic parameters are shown in (Table 3).

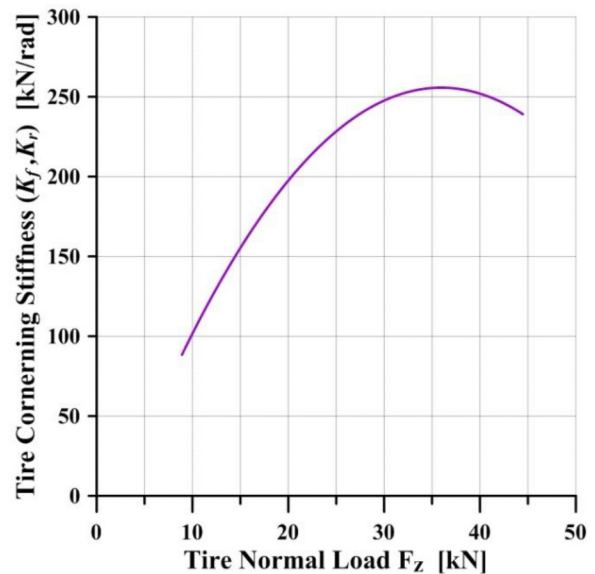


Figure 7. Relation between tire normal load versus cornering stiffness.

Table 2. Bus chassis design parameters.

Overall Length (L)	12.2 m
Frontal Area (A_f)	7.67 m ²
Overall Mass (m)	18000 kg
Distance Between CG and Front Axle (l_f)	3.51 m
Distance Between CG and Rear Axle (l_r)	2.49 m
Yaw Moment Inertia (I_y)	275000 kg.m ²
Front Tire Cornering Stiffness (K_f)	255.61 kN/rad
Rear Tire Cornering Stiffness (K_r)	232.29 kN/rad
Distance between CG and NSP (l_N)	0.36 m

Table 3. Bus aerodynamic parameters.

β_w [°]	C_s [-]	l_w [m]	V_f [m/s]
5 °	0.453	-1.721	2.19
10 °	0.989	-1.684	4.41
15 °	1.510	-1.628	6.70
20 °	2.048	-1.460	9.10
25 °	2.571	-1.258	11.66
30 °	3.101	-1.006	14.43
35 °	3.590	-0.861	17.51
40 °	4.030	-0.765	20.98
45 °	4.209	-0.716	25

5. RESULTS AND DISCUSSION

For the first moment and before discussing model simulation results, all the values of (l_w) are found to be in front of bus CG while (l_N) is behind bus CG. Which means a CCW coupling moment is generated between vehicle internal force ($2\beta(K_f +$

2K_y) and lateral wind gust side force (F_s), i.e., the bus will always tend to CCW yaw motion during simulation. Moreover, while the values of side force coefficient (C_s) increasing with each wind gust velocity (V_i) (from 100 % at $\beta_w = 5^\circ$ to 929 % at $\beta_w = 45^\circ$), the distance between vehicle CG and AC (l_w) is decreasing (from 100 % at $\beta_w = 5^\circ$ to 42 % at $\beta_w = 45^\circ$). Nevertheless, the cross product of yaw moment created due to side force (F_s) and its arm (l_w) is increasing with each wind gust velocity. The wind gust external force (F_s) is prescribed in Eq.(3) and the wind gust external moment is ($l_w F_s$) is prescribed in Eq.(4). Finally, it can be expected that all vehicle lateral dynamic responses are directly proportional with wind gust velocity (V_i).

5.1. Lateral Deviation Response

Figures 8,9,10 are demonstrating the variation in bus model CG lateral deviation (LD) with different wind relative yaw angles (β_w) and their corresponding lateral wind gust velocities (V_i). Lateral deviation (LD) represents the anticipated vehicle path in the lateral direction due to wind gust excitation. A direct proportional relation is observed between lateral deviation (LD) and wind gust velocity (V_i). With increasing in lateral deviation (LD), either vehicle lane unsteady behavior or vehicle lane deviation is obtained. Moreover, with high wind gust velocities, in particular wind gust velocities over 10 m/s, the driver has to pay more attention to maintain vehicle steady lane motion.

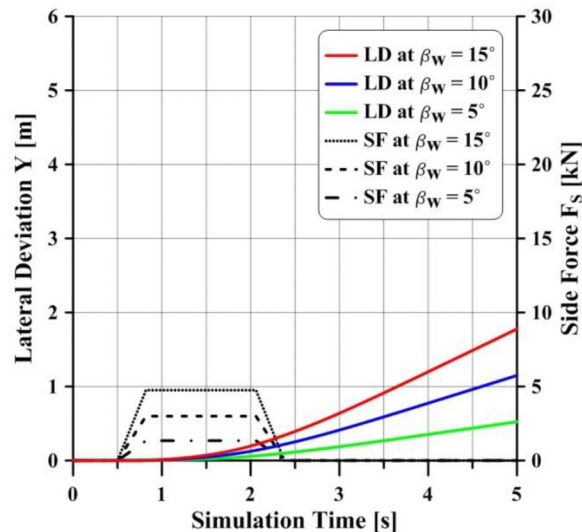


Figure 8. Variation of lateral deviation from $\beta_w = 5^\circ$ to $\beta_w = 15^\circ$.

After one second of applying wind gusts excitation (at ST=1.5 s), a small change in vehicle lateral deviation (LD) value is determined for all wind gust velocities (LD= 0.02 m at $\beta_w = 5^\circ$ and LD= 0.3 m at $\beta_w = 45^\circ$). However, a recognized rising of lateral deviation(LD) curve is reported with increasing in simulation time (ST) for each wind gust velocity. Regarding low

wind gust velocities (Figures 8,9) with $V_i < 10$ m/s (Figure 1c shows the exact relation between (β_w) and wind velocity), the maximum reported value of lateral deviation (LD) at $\beta_w = 20^\circ$ after 2.5 seconds of wind gust excitation (which corresponds ST= 3 s) is less than one meter. The standard highway lane width value [15] is between (3.5 - 3.75 m) and bus width is about 2.5 m [16]. Accordingly, it can be concluded that any wind gust velocity over 10 m/s will lead mostly to course deviation after 2.5 seconds (which corresponds to 85 % of drivers PIEV time [17] without considering vehicle kinematics). The maximum lateral deviation (LD) obtained after 5 seconds of applying an equivalent wind gust velocity to upwind velocity, i.e. at $\beta_w = 45^\circ$, is LD= 5.23 m (Figures 10).

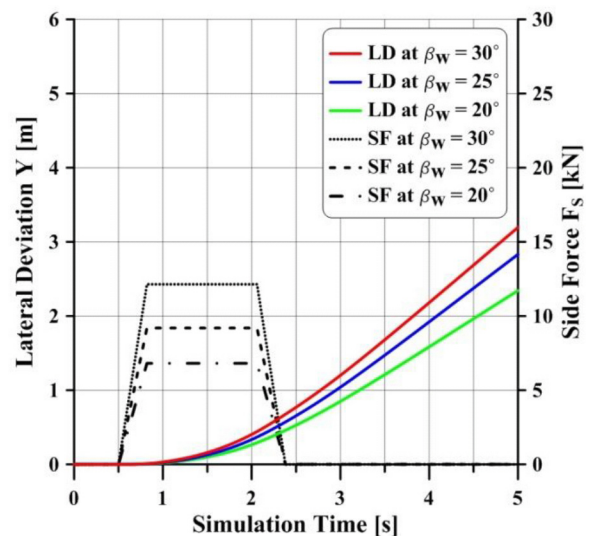


Figure 9. Variation of lateral deviation from $\beta_w = 20^\circ$ to $\beta_w = 30^\circ$.

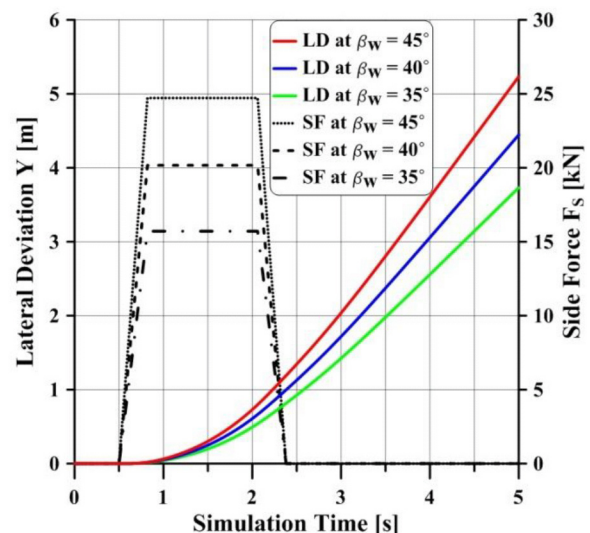


Figure 10. Variation of lateral deviation from $\beta_w = 35^\circ$ to $\beta_w = 45^\circ$.

5.2. Lateral Acceleration Response

Figures 11,12,13 are demonstrating the variation of bus model CG lateral acceleration (LA) with different wind relative yaw angles (β_w) and their corresponding lateral wind gust velocities (V_w). Lateral acceleration (LA) is an indication of vehicle velocity variation in the lateral direction. It affects significantly the driver perception and his reaction to wind gust [9]. Additionally, the ride comfort of a passenger is influenced directly by lateral acceleration (LA) characteristics as evaluated in [18,19]. Lateral acceleration (LA) response behavior depends mainly on wind gust side force (F_s) excitation signal form (e.g., step input, ram input) and vehicle chassis design parameters (e.g., CG position, NSP position, axle tires cornering stiffness).

With increasing in wind gust velocity (V_w), not only variation in lateral acceleration (LA) values but also relatively changes in curve behavior is observed. For the time period elapsed between applying wind gust excitation and before maintaining fully developed wind velocity, a direct proportional relation between lateral acceleration (LA) and wind side force (F_s) is clearly noticed. However different peak values for each lateral acceleration (LA) response is observed, the same direct proportional relation is also observed during collapse of wind gust side force (F_s) from its steady full value to zero. After wind gust side force (F_s) influence period, a post lateral acceleration (LA) is estimated. The post response of lateral acceleration (LA) refers to vehicle chassis design parameters.

As a result of increasing in wind side force (F_s) due to variation in wind gust velocity (V_w), a difference between each wind gust lateral acceleration (LA) peaks ratio (Which is the ratio between maximum values of lateral acceleration (LA) at the start and end of wind gust excitation) is obtained. It is fluctuating between 55 % at $\beta_w = 5^\circ$ to 99 % at $\beta_w = 45^\circ$. This can be explained as a result of increasing in side force (F_s) applied to the bus while bus mass is still constant which increases the lateral acceleration (LA) response in the beginning of wind excitation applying. Moreover, the ratio between the peak value of post lateral acceleration and the maximum obtained value of lateral acceleration (LA) for each wind gust is decreasing from 56 % at $\beta_w = 5^\circ$ to 40 % at $\beta_w = 45^\circ$. While the starting peak of lateral acceleration is increasing, the post lateral acceleration peak is decreasing. They are considered to compensate each other but without the same value. The maximum value of any wind gust lateral acceleration (LA) is always the second peak (at the instant where wind gust starts to collapse) and it is always directly proportional with wind gust velocity (V_w). The maximum reported values of lateral acceleration (LA) are between 0.1 m/s^2 at $\beta_w = 5^\circ$ and 0.95 m/s^2 at $\beta_w = 45^\circ$.

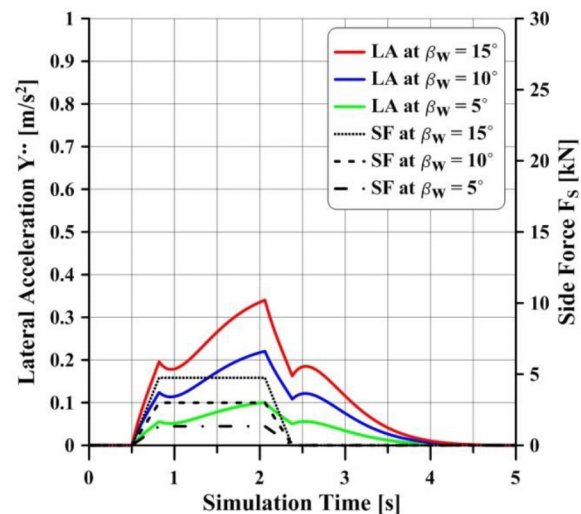


Figure 11. Variation of lateral acceleration from $\beta_w = 5^\circ$ to $\beta_w = 15^\circ$.

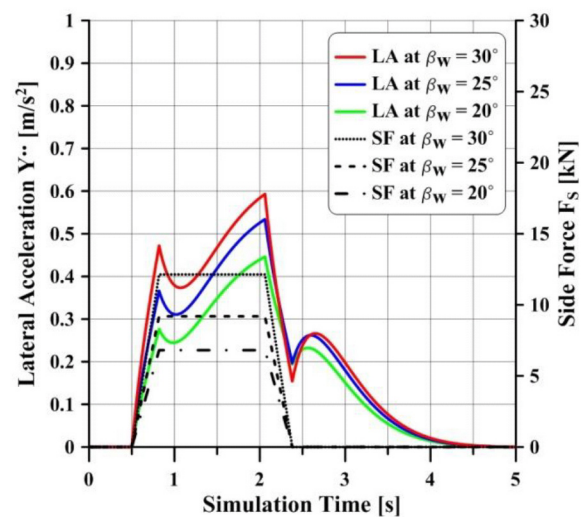


Figure 12. Variation of lateral acceleration from $\beta_w = 20^\circ$ to $\beta_w = 30^\circ$.

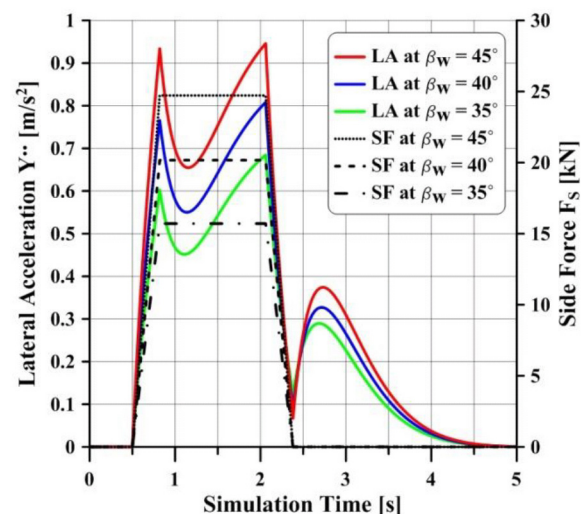


Figure 13. Variation of lateral acceleration from $\beta_w = 35^\circ$ to $\beta_w = 45^\circ$.

5.3. Yaw Angle Response

Figures 14, 15, 16 are demonstrating the variation of bus model CG yaw angle (YA) with different wind relative yaw angles (β_w) and their corresponding lateral wind gust velocities (V_l). Definitely, the Yaw angle (YA), vehicle heading angle, is an indication of vehicle directional stability under given excitation. Due to vehicle tires cornering stiffness forces and the distance between CG and NSP (l_N), an additional yaw angle is produced during vehicle cornering maneuvers. Basically, this additional yaw angle is responsible for vehicle under-steer or over-steer behaviors. The presented lateral vehicle dynamics analysis has no driver steering angle (fixed steering wheel), however, a lateral wind gust side force (F_s) excitation is responsible for generating yaw angle (YA). Since any road vehicle is influenced directly by any lateral excitation (e.g., wind side force, cornering maneuver centrifugal force), the driver has to compensate continuously to achieve a steady heading direction as straight ahead in the middle of driving lane.

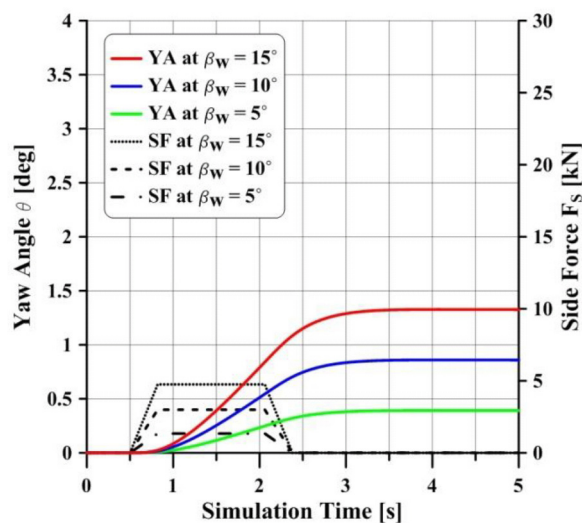


Figure 14. Variation of yaw angle from $\beta_w = 5^\circ$ to $\beta_w = 15^\circ$.

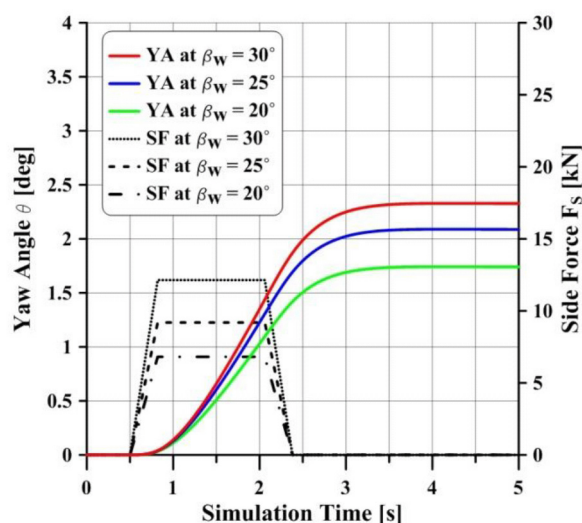


Figure 15. Variation of yaw angle from $\beta_w = 20^\circ$ to $\beta_w = 30^\circ$.

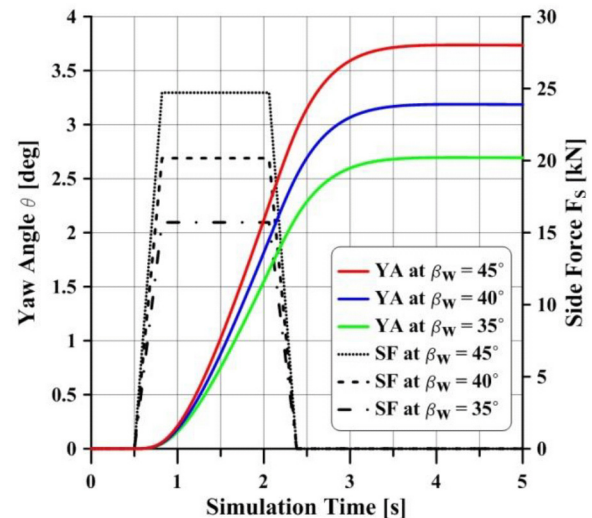


Figure 16. Variation of yaw angle from $\beta_w = 35^\circ$ to $\beta_w = 45^\circ$.

With increasing in wind gust velocity (V_l), the maximum attained yaw angle response is increasing also. In the first 0.3 seconds of imposing lateral wind gust (at $ST = 0.7$ s), a negligible yaw rate response (YA) is reported for all wind gusts (which refers to bus yaw inertia). However, while applying wind gust excitation (remaining influence period), the yaw angle response (YA) is increasing. Moreover, a less rising tendency is noticed after the collapse of wind gust side force (F_s). After three seconds of applying wind gust (at $ST = 3.5$ s), a settling value of each yaw angle response (YA) is maintained. The settled yaw angle response (YA) is increasing with wind gust velocity (V_l) from $YA = 0.38^\circ$ at $\beta_w = 5^\circ$ to $YA = 3.74^\circ$ at $\beta_w = 45^\circ$. Regarding high wind gust velocities (Figures 15, 16) and, in particular, with $V_l > 10$ m/s (Figure 1c) during the first one and half seconds of applying wind gust (at $ST = 2$ s), all the estimated values of yaw angle responses (YA) is greater than 1 degree. Additionally, the steering ratio for such commercial vehicle is more than 20:1 [20]. Without considering steering system kinematics and vehicle-driver interaction transient characteristics, a higher driver response is required to compensate high wind gusts induced yaw angle (YA).

5.4. Yaw Rate Response

Figures 17, 18, 19 are demonstrating the variation of bus model CG yaw rate (YR) with different wind relative yaw angles (β_w) and their corresponding lateral wind gust velocities (V_l). Definitely, Yaw rate (YR) is an important parameter to judge vehicle stability. On the other hand, the driver response to wind gust is depending, with much weight, on his perception of vehicle yaw rate (YR) [9]. Basically, yaw rate is much concerned during cornering maneuvers which are not applicable for the current case (fixed steering wheel). According to current simulation criteria, yaw rate (YR) represents the variation in heading direction (due to lateral wind gust excitation) as a function of time. Moreover, many researchers have investigated different control strategies for

yaw rate (YR) which has been considered as an important parameter for evaluating vehicle stability and handling characteristics [21,22].

With increasing in wind gust velocity (V_f), the maximum attained yaw rate is increasing also. However different wind gusts, a similar yaw rate (YA) behavior is observed but with different values. During influence period of wind gust excitation and before breakdown, a direct proportional relation between yaw rate (YR) and wind gust side force (F_s) is estimated. The peak value of all yaw rates is obtained before side force breakdown, thereafter, a dramatically fall is noticed till reach zero at about ST= 4 s. After one second of applying wind gusts excitation (at ST= 1.5 s), the maximum reported value of low wind gust velocities ($V_f < 10$ m/s Figure 1c) yaw rates is about 1 deg/s (Figures 17,18). However, a double yaw rate (YR) response is attained at $V_f = 25$ m/s for the same time (Figure19). Additionally, the maximum concluded values of yaw rate (YR) are between 0.25 deg/s at $\beta_w = 5^\circ$ and 2.33 deg/s at $\beta_w = 45^\circ$.

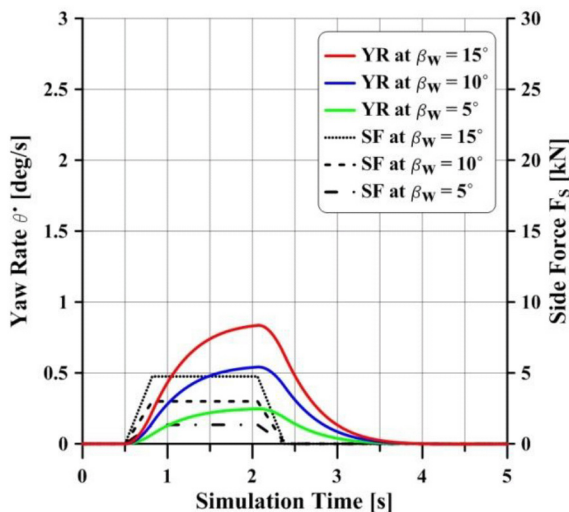


Figure 17. Variation of yaw rate from $\beta_w = 5^\circ$ to $\beta_w = 15^\circ$.

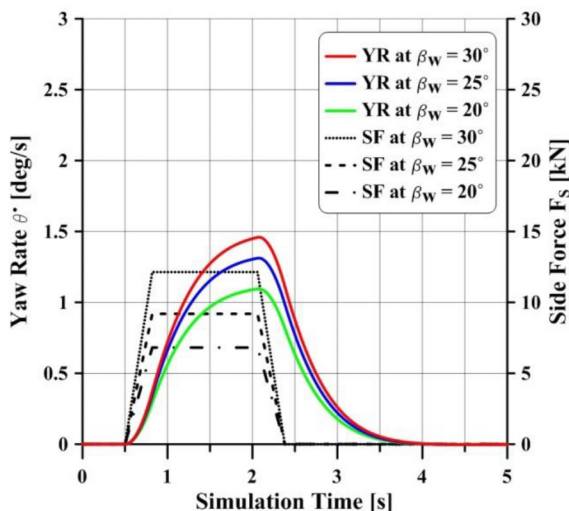


Figure 18. Variation of yaw rate from $\beta_w = 20^\circ$ to $\beta_w = 30^\circ$.

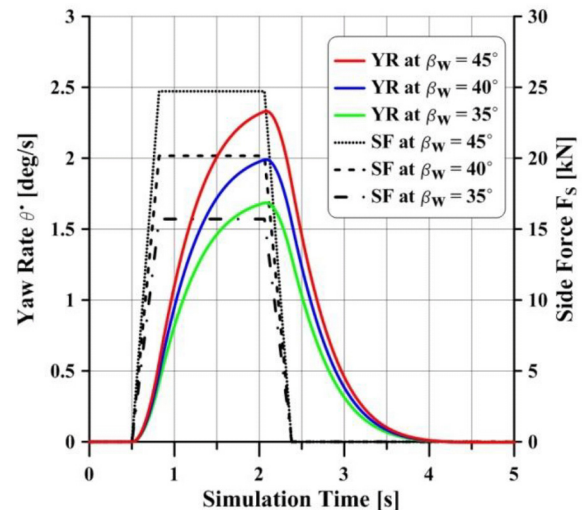


Figure 19. Variation of yaw rate from $\beta_w = 35^\circ$ to $\beta_w = 45^\circ$.

CONCLUSIONS

The effect of wind gusts variety on a commercial vehicle had been modeled. The four lateral vehicle dynamic common parameters (LD, LA, YA, YR) are intensively investigated. Lateral vehicle dynamic responses are concluded to be function in wind side force (F_s) and its arm (l_w). The influence of high wind gust velocities ($V_f > 10$ m/s Figure 1c) on bus lateral dynamics is clearly critical. A limited vehicle lateral dynamic responses are obtained under wind gust velocities of 10 m/s. Both lateral deviation (LD) and yaw angle (YA) maintained their maximum values at the end of simulation time, however, lateral acceleration (LA) and yaw rate (YR) attained their peak values at point before wind gust side force (F_s) breakdown. In order to maintain a good level of vehicle handling and stability without high expenses, a pre-manufacturing evaluation of vehicle response to variable wind gusts is required. The coupled analysis between vehicle lateral dynamics and vehicle aerodynamics introduced itself as important technique to assess vehicle expected behaviors in wind gusts, in particular, at the primary design stages.

REFERENCES

1. Mansor, S., and Passmore, M.A., "Effect of Rear Slant Angle on Vehicle Crosswind Stability Simulation on a Simplified Car Model," International Journal of Automotive Technology (4):1701-706, 2013, doi:10.1007/s12239-013-0076-1.
2. Favre, T., Diedrichs, B., and Efraimsson, G., "Detached-Eddy Simulations Applied to Unsteady Crosswind Aerodynamics of Ground Vehicles," Third Symposium on Hybrid RANS-LES Methods, 2009, doi:10.1007/978-3-642-14168-3_14.
3. Favre, T., "Aerodynamics simulations of ground vehicles in unsteady crosswind," Ph.D. thesis, KTH, School of Engineering Sciences (3-5), Stockholm, Sweden, 2011.
4. Brondolo, L., "Comparative Investigation of Large Eddy Simulation and RANS Approaches for External Automotive Flows," M.Sc. thesis, School of Engineering Cranfield University, Cranfield (96-98), UK, 2011.
5. Hemida, H., and Kranovic, S., "DES of the Flow Around a Realistic Bus Model Subjected to a Side Wind with 30 Degree Yaw Angle," presented at The Fifth IASME/WSEAS International Conference on Fluid Mechanics and Aerodynamics 2007, Athens, Greece, August 25-27, 2007.

6. ANSYS® Academic Research, Release 14.0, Help System, FLUENT Theory guide, ISBN 7247463304:1-136, 2011.
 7. William, Y.E., Mohamed, M.H., and Oraby, W.A.H., "Investigation of Crosswind Aerodynamics for Road Vehicles Using CFD Technique," presented at Eleventh International Conference of Fluid Dynamics 2013 (ICFD11-EG-4003), Alexandria, Egypt, December 19-21, 2013.
 8. Abe, M., "Vehicle Handling Dynamics," first edition, Elsevier, UK, ISBN 9780080961811:56-146, 2009.
 9. Hucho, W. H., "Aerodynamics of Road Vehicles," Fourth edition, SAE International, ISBN 0768000297:268-760, 1998.
 10. Nakashima, T., Tsubokura, M., Vázquez, Owen, H., and Doi, Y., "Coupled analysis of unsteady aerodynamics and vehicle motion of a road vehicle in windy conditions," ELSEVIER Computer & Fluids (80):1-9, 2013, doi:10.1016/j.compfluid.2012.09.028.
 11. Docton, M.K.R., "The Simulation of Transient Cross Winds on Passenger Vehicles," Ph.D. thesis, School of Engineering University of Durham (142-150), Durham, UK, 1996.
 12. MathWorks®, Release R2014a, Simulink Reference, 2014.
 13. Juhlin, M., "Assessment of crosswind performance of buses," Ph.D. thesis, KTH, School of Engineering Sciences (27-51), Stockholm, Sweden, 2009.
 14. Balderas, L., and Fancher, P., "Representation of Truck Tire Properties in Braking and Handling Studies: The Influence of Vertical Load on Side Force," MVMA project No. 8168, The University of Michigan Transportation Research Institute, Michigan, USA, August 1988.
 15. TEM STANDARDS AND RECOMMENDED PRACTICE, Third Edition February 2002.
 16. Hjort, M., and Jansson J., "Handling of buses on slippery roads during the influence of side wind: a study of the effects of different tyres," ELSEVIER Accident Analysis and Prevention (42):972-977, 2010, doi:10.1016/j.aap.2009.04.011.
 17. AASHTO, "Policy on Geometric Design of Streets and Highways," Washington, DC, 1984, 1990, and 1994.
 18. Xu, Y.L., and Guo, W.H., "Effects of bridge motion and crosswind on ride comfort of road vehicles," ELSEVIER Journal of Wind Engineering and Industrial Aerodynamics (92): 641-662, 2004, doi:10.1016/j.jweia.2004.03.009.
 19. Beard, G. F., and Griffin, M.J., "Discomfort during lateral acceleration: Influence of seat cushion and backrest," ELSEVIER Applied Ergonomics (44):588-594, 2013, doi:10.1016/j.apergo.2012.11.009.
 20. Blundell, M., and Harty, D., "Multibody Systems Approach to Vehicle Dynamics," First edition, ELSEVIER, ISBN 0750651121:363-368, 2004.
 21. Mirzaei, M., "A new strategy for minimum usage of external yaw moment in vehicle dynamic control system," ELSEVIER Transportation Research Part C (18):213-224, 2010, doi:10.1016/j.trc.2009.06.002.
 22. Du, H., Zhang, N., and Naghdy, F., "Velocity-dependent robust control for improving vehicle lateral dynamics," ELSEVIER Transportation Research Part C (19):454-468, 2011, doi:10.1016/j.trc.2010.05.004.
- I_f - Distances from vehicle CG to the front axle (m).
 I_N - Distance between vehicle CG and NSP (m).
 I_r - Distances from vehicle CG to the rear axle (m).
 I_w - Distance between vehicle CG and AC (m).
 L_M - Vehicle model overall length (m).
 L_w - Distance between AC and vehicle model rear end (m).
 m - Vehicle mass (kg).
 V - Vehicle velocity or upwind velocity (m/s).
 V_l - Lateral wind gust velocity (m/s).
 V_w - Resultant imposed wind velocity (m/s).
 X, Y - Absolute coordinates of vehicle's CG (m).
 \ddot{Y} (d^2y/dt^2) - Vehicle lateral acceleration (m/s²).
 β - Resultant vehicle side slip angle (rad).
 δ - Front wheel steer angle (rad).
 θ - Vehicle yaw angle (rad).
 $\dot{\theta}$ ($d\theta/dt$) - Vehicle yaw rate (rad/s).
 ρ_{air} - Air density = 1.225 (kg/m³).
AC - Aerodynamic center.
CCW - Counterclockwise.
CFD - Computational fluid dynamics.
CG - Center of gravity.
CW - Clockwise.
DOF - Degree of freedom.
LA - Lateral acceleration.
LD - Lateral deviation.
NSP - Neutral steer point.
PIEV - Perception, intellection, emotion and volition (the amount of time taken by a driver for hazard reaction).
SF - Side force.
SIMPLE - Semi-implicit method for pressure linked equation
ST - Simulation time.
YA - Yaw angle.
YR - Yaw rate.

DEFINITIONS/ABBREVIATIONS

- A_f - Vehicle frontal area (m²).
Cs - Aerodynamic side force coefficient (-)
 F_s - Aerodynamic side force acting on the vehicle (N).
 F_z - Tire normal load (N).
 I_z - Vehicle yaw moment inertia (kg.m²).
 K_f, K_r - Cornering stiffness of front and rear tires (N/rad).
 l - Wheel base (m).

All rights reserved. No part of this publication may be reproduced, stored in a retrieval system, or transmitted, in any form or by any means, electronic, mechanical, photocopying, recording, or otherwise, without the prior written permission of SAE International.

Positions and opinions advanced in this paper are those of the author(s) and not necessarily those of SAE International. The author is solely responsible for the content of the paper.